

Original citation:

Dinh, T. Q., Marco, James, Greenwood, D., Harper, L. and Corrochano, D. (2016) Powertrain modelling and engine start control of construction machines. In: 3rd International Conference on Powertrain Modelling and Control Testing, Mapping and Calibration, Loughborough University, UK, 7-9 Sep 2016

Permanent WRAP URL:

<http://wrap.warwick.ac.uk/81454>

Copyright and reuse:

The Warwick Research Archive Portal (WRAP) makes this work by researchers of the University of Warwick available open access under the following conditions. Copyright © and all moral rights to the version of the paper presented here belong to the individual author(s) and/or other copyright owners. To the extent reasonable and practicable the material made available in WRAP has been checked for eligibility before being made available.

Copies of full items can be used for personal research or study, educational, or not-for-profit purposes without prior permission or charge. Provided that the authors, title and full bibliographic details are credited, a hyperlink and/or URL is given for the original metadata page and the content is not changed in any way.

A note on versions:

The version presented here may differ from the published version or, version of record, if you wish to cite this item you are advised to consult the publisher's version. Please see the 'permanent WRAP URL' above for details on accessing the published version and note that access may require a subscription.

For more information, please contact the WRAP Team at: wrap@warwick.ac.uk

Powertrain Modelling and Engine Start Control of Construction Machines

T.Q. Dinh^{1,*}, J. Marco¹, D. Greenwood¹, L. Harper², D. Corrochano²

¹WMG, University of Warwick, Coventry CV4 7AL, UK; james.marco@warwick.ac.uk;
d.greenwood@warwick.ac.uk

²JCB, Rocester, Staffordshire, ST14 5JP, UK; lee.harper@jcb.com; david.corrochano@jcb.com

* Correspondence: q.dinh@warwick.ac.uk; Tel.: +44-2476-574902

Abstract: This paper aims to develop an engine start control approach for a micro/mild hybrid machine for a capable of cranking the engine without injection. First, the powertrain is physically modelled using a co-simulation platform. Second, experiment data of the traditional machine is acquired to optimize the model. Third, a model-based adaptive controller is designed for the starter to crank the engine quickly and smoothly to minimize the operator discomfort. The effectiveness of the proposed approach is validated through numerical simulations with the established model.

Keywords— Construction machine, modelling, optimization, start control.

1-Introduction

Construction industry is ranked third just behind oil and gas and chemical manufacturing sectors in terms of having influence on the greenhouse effect. Additionally, energy crisis becomes more and more serious in recent years while fuel consumption of these equipment accounts for a significant portion of total global fuel usage. Thus, improving efficiency of construction equipment is very important and is one of the key factors for creating a clean environment and saving energy.

There have been much effort in research on hybridization technologies in terms of fuel economy and environmental impacts for various applications ranging from transportation to construction equipment. Micro/mild hybridisation, which has been widely used for modern vehicles, is known as a feasible solution with high fuel efficiency, less emission and especially, low cost and easy installation regardless of drivetrain configuration. For a micro/mild hybrid system, one of the most significant factors affecting the overall performance is known as engine start/stop operation. There is a number of studies on engine start/stop control for both conventional vehicle [1] and hybrid vehicles [2]. Although the engine performance could be improved using the suggested methodologies, the control optimizations were the complex processes which only could be carried out offline. Therefore, these control approaches lack of adaptability for real-time applications such as engine start operation where there are large numbers of nonlinearities and uncertainties. To the best of our knowledge on construction sector, the development of start/stop control for micro/mild

hybrid equipment is still limited. Herein to save energy, two important tasks are an engine start control approach and, determination of engine idle state to define when the engine can be switched to idle or turned off [3, 4]. To address the first task, a controller needs to be properly designed to start the engine quickly and smoothly to reduce impacts of machine noise, vibration and harshness (NHV), due to large inertia and peak compression torque of the engine, on the driver comfort.

This paper focuses on the design of engine start control for micro hybrid construction machines. Powertrain of a typical excavator has been selected for the study. Here, the traditional starter is replaced with a larger electric motor for a capable of cranking the engine directly from zero speed without the use of injection. First, the powertrain is physically modelled using AMESim and then, embedded into Simulink to perform the co-simulation platform. Second, experiment data with the selected machine is acquired to optimize the model. Third based on the optimized model, a model-based adaptive controller which is the combination of an inverse model and a proportional-integral (PI)-based adaptive controller is constructed to drive the starter to enhance the quick and smooth engine start. Simulations have been carried out to evaluate the capability of the designed controller.

2-Powertrain Architecture and Co-Simulation Platform

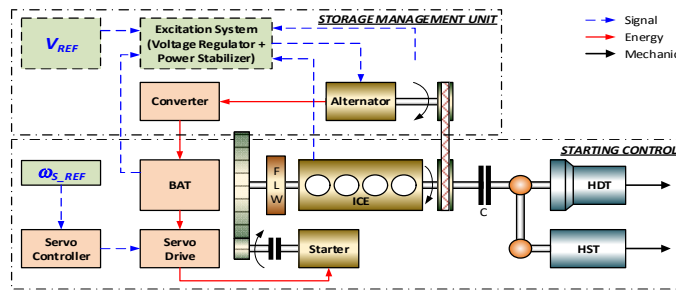


Fig. 1. Powertrain configuration of a generic construction machine

The powertrain architecture of a generic machine can be described in Fig. 1. Here, the power system mainly consists of the ICE, starter and alternator. The starter is engaged to the engine using the pinion-ring gear mechanism (integrated a flywheel) via an over-running clutch. The output shaft of the engine is coupled to the alternator with a belt transmission. The electricity created by the alternator is stored in the battery which is used to supply power for the starter. The drivetrain, work hydraulics and other auxiliaries are assumed as a combination of a hydrodynamic transmission and a hydrostatic transmission connected to the engine output shaft through a clutch. These parts can be simplified as a dynamic load simulator with adjustable inertia. For engine start control, this dynamic load can be neglected or approximated as a small constant load.

Due to the need to characterise the powertrain behaviour and to support for the control design, it is necessary to develop an accurate and complete model. However due to the system with high nonlinearities and uncertainties, especially with the engine dynamics, the modelling process could be significantly complex. In order to overcome this problem, a co-simulation platform using

AMESim and MATLAB/Simulink is suggested. AMESim is the advanced simulation tool which provides sufficient libraries for physical modelling approaches which eliminate the tedious mathematical modelling, code programming while ensure high modelling efficiency [5]. The main drawback of using AMESim is control system design. Meanwhile, MATLAB/Simulink is the powerful tool for control system design, modelling and optimization. Thus, the co-simulation using these tools is a feasible solution for powertrain modelling and control.

3-Powertrain Modelling

3.1-Engine Model

The four-stroke diesel engine model was firstly constructed to estimate the engine transient response. As shown in Fig. 2(a), this engine block mainly includes following components: four combustion cylinders which were linked together to a crankshaft; intake and exhaust mechanisms with compressor, intercooler, throttle and exhaust gas recirculation (EGR).

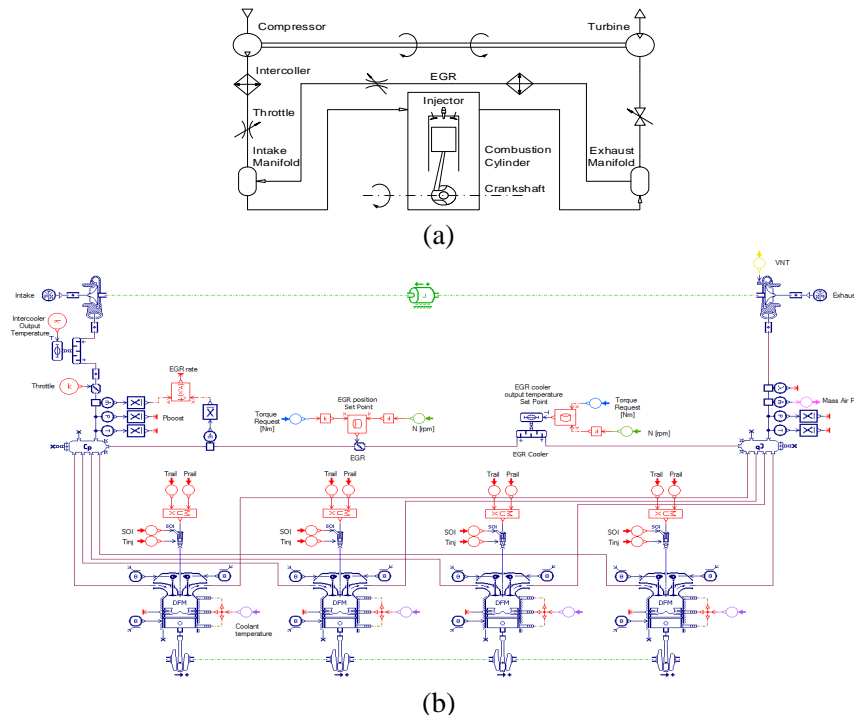


Fig. 2. Four-stroke internal combustion engine: (a) Configuration; (b) Model built in AMESim

By using AMESim and thermodynamic analysis [7-8], the engine physical model was built as in Fig. 2(b). To estimate the engine transient behaviour, the model inputs can be listed as:

- Combustion cylinder: coolant temperature, temperature and pressure of the injected fuel, start of injection and injection duration

- Intake and exhaust mechanisms: intercooler control signal throttle control signal, variable geometry turbine position, engine torque request, engine speed

3.2-Starter, Alternator and Battery Models

Electric components in the powertrain used for the engine cranking operation are a DC motor with direct current drive, a DC output generator and a lead-acid battery. By using AMESim, the equivalent electrical circuit of a direct current machine with permanent excitation was used to model this motor in which the inputs are temperature, supply voltage and load torque, and the outputs are current and rotational speed. Meanwhile, the alternator with DC output was represented as an average model of current generator with external voltage regulation. The model inputs are temperature, rotational speed, storage voltage and desired voltage while the outputs are torque and storage current. The lead-acid battery was modelled by an equivalent electric circuit of variable voltage source and variable resistance which are function of the state of charge (SOC) and temperature. These component models are shown in Fig. 3.

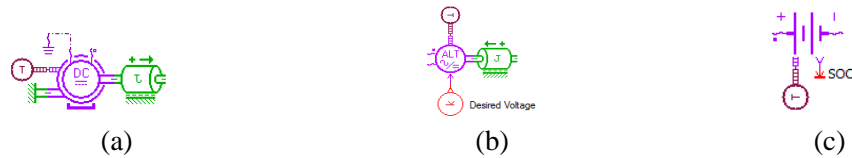


Fig. 3. Electric component models: (a) Starter motor; (b) Alternator; (c) Battery

3.3-Transmission and Load Models

The pinion-ring gear mechanism was modelled as a gear transmission connected to a controllable clutch. Additionally, the integrated flywheel was presented by a constant rotary load while all the friction losses through this transmission was presented by a friction mean effective pressure model (Fig. 4(a)). By assuming that there was no extension or damage of belt, the belt transmission model was a set of a two-input-one-output rotary node, a gear transmission with fixed ratio and a rotary spring-damper as in Fig. 4(b). As mentioned in Section 2, the loads at the engine output shaft could be represented by a constant small rotary load with another rotary spring-damper (Fig. 4(c)). As a result, the powertrain model was completely build as displayed in Fig. 5.

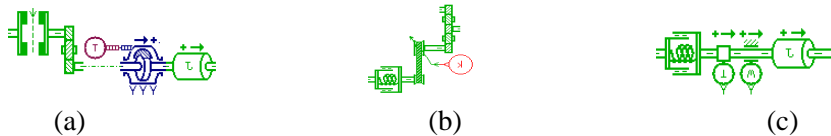


Fig. 4. Transmission and load models: (a) Gear transmission; (b) Belt transmission; (c) Loads

3.4-Power System Control Signal and Logics

The control signals and logics designed for the power system model as shown in Fig. 6 consist of:

- Input signals: key On/Off event, pedal position, and engine torque command which were achieved from experiments with the excavator

- Engine speed controller bases on the input signals and current engine speed to define the engine torque request and engine modes. Here, the engine operation was basically classified into four modes: engine start with injection, injection off, idle, and normal power.
- Engine control unit uses the defined mode to control the combustion process with air flow, rail pressure and injection.
- Starter control unit: in case of traditional design, there was only the direct connection between the motor and power supply models. An electric switch was used to turn on or off this motor. Conversely in micro hybrid model, the motor speed was controlled by the proposed controller, build in Simulink, via the inverter model.

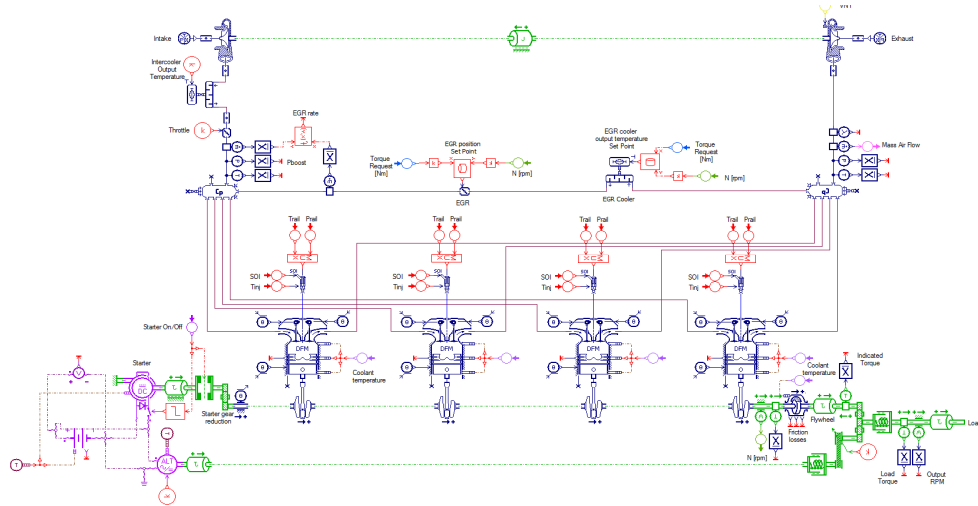


Fig. 5. Complete powertrain model of a generic construction machine built in AMESim

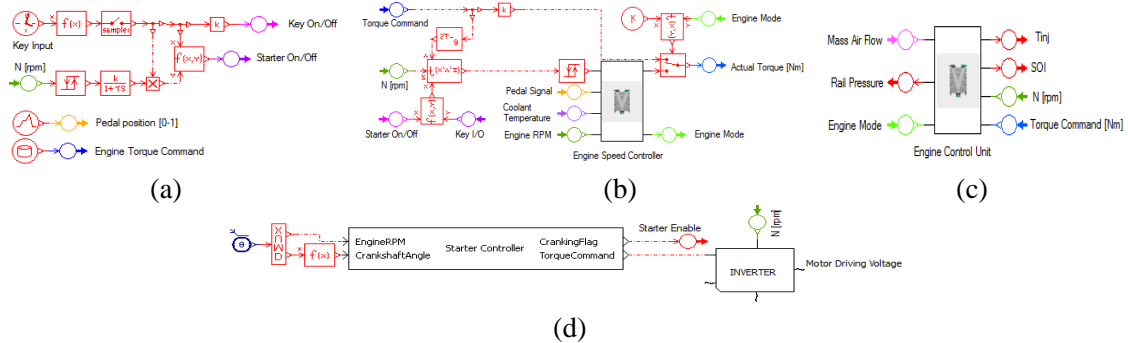


Fig. 6. Model's control: (a) Inputs; (b) Engine speed controller; (c) Engine control unit; (d) starter control unit

4-Model Optimization

As the next step, parameters of the designed model need to be identified. The key parameters as well as the source for setting their initial values are listed in Table 1.

Table 1 – Model parameters and sources for parameter setting and optimization

Components	Parameters	Source for Initial Values	Source for Optimization
Belt	Pulley diameters, D_{p1}, D_{p2} Pulley moment of inertia, I_{p1}, I_{p2} Belt damping coefficient and stiffness, c_B, k_B	Manufacturer	Experiment Experiment
Engine mechanism	Crank arm length, R_{crank} Rod length, L_{rod} , cylinder: bore diameter, D_{bore} , clearance, L_{clear} Compression ratio, C_{com} , stroke, S_{cyl} Equivalent engine inertia, I_E Static and dynamic friction parameters	Geometry Geometry Geometry Geometry AMESim	Experiment Experiment
Engine thermodynamics	Fuel density, ρ_f , Specific heat ratio, γ Numbers of moles of gas, n_g , Fuel lower heating value, LHV_f Crank angle at the start of the premixed and diffusion phases of combustion, Duration of these phases Weibe parameter set	AMESim AMESim Manufacturer AMESim	Experiment Experiment Experiment Experiment
Pinion-ring gear	Transmission ratio, R_G , transmission efficiency, η_G Pinion and ring gear geometric parameters Flywheel moment of inertia, I_F	Manufacturer Geometry Geometry	Experiment Experiment
Starter motor	Resistant load, R_S , armature conductance, L_S , armature gain, k_S Rotor moment of inertia, I_S	AMESim Geometry	Experiment
Alternator	Rotor moment of inertia, I_A Other dynamics	Geometry AMESim	Experiment
Battery	Number of cells, Nominal capacity Resistance	Manufacturer AMESim	Experiment

Table 2 – Procedure and method for powertrain model optimization

Step	Test Conditions	Model Input / Output and Data	Method
Step 1 - Parameterization and validation for Starter – Engine model	<ul style="list-style-type: none"> Without injection Without connecting to alternator 	<ul style="list-style-type: none"> Input: key event Output: battery output voltage 	Parameter estimation toolbox for optimizing parameters of battery, starter, starter-engine inertia
Step 2 - Parameterization and validation for Starter – Engine – Alternator model	<ul style="list-style-type: none"> Without injection 	<ul style="list-style-type: none"> Input: key event Output: battery output voltage 	Parameter estimation toolbox for optimizing parameters of alternator inertia
Step 3 - Parameterization and validation for full powertrain model	<ul style="list-style-type: none"> Connecting all component Injection was enabled 	<ul style="list-style-type: none"> Input: engine torque Output: engine speed 	Parameter estimation toolbox for optimizing parameters of combustion process (thermal dynamics)

Based on Table 1, the powertrain model was optimized using the nonlinear least square-based parameter estimation and the experimental data. The procedure to optimize the powertrain model was performed with three steps as shown in Table 2. Here, the experiments in Table 2 were cranking tests with the researched excavator in the normal working temperature, around 25°C. The starter was firstly activated to rotate the engine from zero rpm to 200rpm and then, the injection was enabled to crank the engine to an idle speed of 850rpm. All the necessary data sets were acquired through CAN bus using mean value calculation method. Figure 7(a) shows the optimization result of the powertrain model by comparing with the actual cranking profile. Another cranking test was done to validate this optimized model and subsequently, the comparison result is

plotted in Fig. 7(b). The results imply that the model has enough capability to estimate the powertrain dynamics.

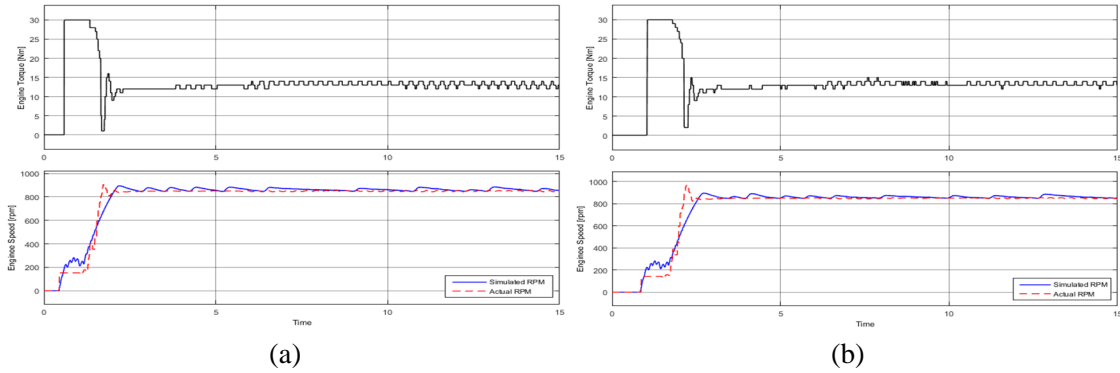


Fig. 7. Modelling result using the powertrain model: (a) Optimization result; (b) Validation result

5-Engine Start Controller

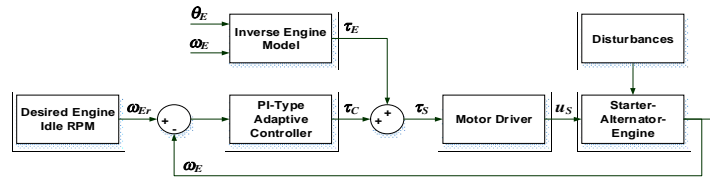


Fig. 8. Proposed model-based control architecture for engine start

The proposed engine start controller is described in Fig. 8. From Section 4, the optimized model of the traditional powertrain could simulate well the cranking performance and therefore, it is useful for powertrain dynamics investigation. However for control applications, this complex model is hardly to be used. In order to build the proposed controller for the micro hybrid powertrain using the larger starter, the powertrain model was simplified and utilized as following steps:

- Step 1: the AMESim model was packaged as a black-box model and embedded into Simulink as an S-function with a mask of the key parameters;
- Step 2: a linear model is derived using a set of the Simulink model input-output data and identification toolbox of MATLAB;
- Step 3: an inverse model was created in which the model inputs are the engine speed and crankshaft angle while the output is the estimated load torque applied to the starter motor shaft.

Hence, the inverse model was capable of reducing the influence of dynamic load torque on the starter motor. Next, the PI-based adaptive controller was constructed to ensure the speed tracking performance of the motor. This adaptive controller was built in a form of PI algorithm using a simple neural network of which the network weights could be tuned online by a Lyapunov stability constrain. Here, the PI-type neural network was generally built for a system with one control input,

u , and n outputs (in this case, $u \equiv \tau_c$; $n=1$). This network consists of three layers: an input layer as a control error sequence $e_k^{NN} = \{e_k^1, \dots, e_k^{n-1}\}$, $e_k^i = y_k^{desired,i} - y_k^{actual,i}$, a hidden layer with two nodes, P and I, following PI algorithm, and an output layer to compute the control input. Define $\{w_k^{Pi}, w_k^{Ii}\}$ is a weight vector of the hidden nodes with respect to input i^{th} , and $\{w_k^P, w_k^I\}$ is the weight vector of the output layer. Therefore, the output from each hidden node is derived based on PI algorithm:

$$O_k^P = \sum_{i=1}^{n-1} w_k^{Pi} e_k^i : \text{Node P}; O_k^I = O_{k-1}^I + \sum_{i=1}^{n-1} w_k^{Ii} e_k^i : \text{Node I} \quad (1)$$

Then, the output from the network is obtained using a linear function:

$$u_k = f(O_k^{NN}) \equiv O_k^{NN} = w_k^P O_k^P + w_k^I O_k^I \quad (2)$$

To ensure the robust control performance, the back-propagation algorithm based on the Lyapunov stability condition was derived to tune the network weights. Define a prediction error function as

$$E_k^{NN} = 0.5 \sum_{i=1}^{n-1} (y_k^{desired,i} - y_k^{actual,i})^2 = 0.5 \sum_{i=1}^{n-1} (e_k^i)^2 \quad (3)$$

By letting $\{w_k^P, w_k^I\}$ to unit, the hidden weights can be online tuned for each step, $(k+1)^{th}$, as follows:

$$w_{k+1}^{Pi \text{ or } Ii} = w_k^{Pi \text{ or } Ii} - \eta_k^{Pi \text{ or } Ii} \frac{\partial E_k^{NN}}{\partial w_k^{Pi \text{ or } Ii}} \quad (4)$$

where η_k^{Pi}, η_k^{Ii} are learning rates within $[0,1]$; the other factors in (4) are derived using partial derivative of the function (3) with respect to each decisive parameter and chain rule method [9].

Lyapunov stability condition: by selecting properly the learning rates $\eta_k^{Pi} \equiv \eta_k^{Ii} = \eta_k$ for step $(k+1)^{th}$ to satisfy (5), then the stability of the PI-based adaptive controller is guaranteed.

$$\sum_{i=1}^{n-1} (e_k^i F_k + 0.5 F_k^2 \eta_k) \leq 0 \quad (5)$$

$$F_k = - \sum_{j=1}^{n-1} \left(\frac{e_k^j}{w_k^{Pi}} \frac{\partial E_k^{NN}}{\partial w_k^{Pj}} + \frac{e_k^j}{w_k^{Ii}} \frac{\partial E_k^{NN}}{\partial w_k^{Ij}} \right).$$

Proof: by defining a Lyapunov function as (6), the change of this function is derived as (7)

$$V_k^{NN} = 0.5 \sum_{i=1}^{n-1} (y_k^{desired,i} - y_k^{actual,i})^2 = 0.5 \sum_{i=1}^{n-1} (e_k^i)^2 \quad (6)$$

$$\begin{aligned} \Delta V_{k+1}^{NN} &= 0.5 \sum_{i=1}^{n-1} \left((e_{k+1}^i)^2 - (e_k^i)^2 \right) \\ &= \sum_{i=1}^{n-1} \left(e_k^i \Delta e_k^i + 0.5 (\Delta e_k^i)^2 \right), \quad (e_{k+1}^i = e_k^i + \Delta e_k^i). \end{aligned} \quad (7)$$

From the PI-based controller structure, one has:

$$\Delta e_k^i = \sum_{j=1}^{n-1} \left(\frac{\partial e_k^i}{\partial w_k^{pj}} \Delta w_k^{pj} + \frac{\partial e_k^i}{\partial w_k^{lj}} \Delta w_k^{lj} \right). \quad (8)$$

Terms $\Delta w_k^{pj}, \Delta w_k^{lj}$ are from (4). By using partial derivative and selecting $\eta_k^{pj} \equiv \eta_k^{lj} = \eta_k$, (8) becomes:

$$\Delta e_k^i = \eta_k F_k. \quad (9)$$

From (9), (7) is rewritten as

$$\Delta V_{k+1}^{NN} = \sum_{i=1}^{n-1} \left(e_k^i F_k + 0.5 F_k^2 \eta_k \right). \quad (10)$$

The tracking performance is guaranteed to be stable only if $\Delta V_{k+1}^{NN} \leq 0, \forall k$. It is clear that except η_k , the other factors in (10) can be determined online based on the prediction error and the chain rule method [9]. Hence for each working step, it is easy to select a proper value of η_k to make (5) satisfy. Therefore, the proof is completed.

6-Simulation Results

Numerical simulations with transient responses during engine start using the tradition concept with starter-injector and the hybrid concept with only the controlled starter have been carried out. Here, the desired cranking speed was 850rpm. A comparison of the simulation results has been made as plotted in Fig. 9. The comparison indicates convincingly that the engine was start quickly and smoothly by using only the starter and model-based adaptive controller. The influence of engine dynamics was reduced by the inverse engine model while the desired speed was guaranteed by the adaptive feedback control. As a result, the NVH performance could be well managed and therefore, the driver comfort as well as fuel economy could be improved.

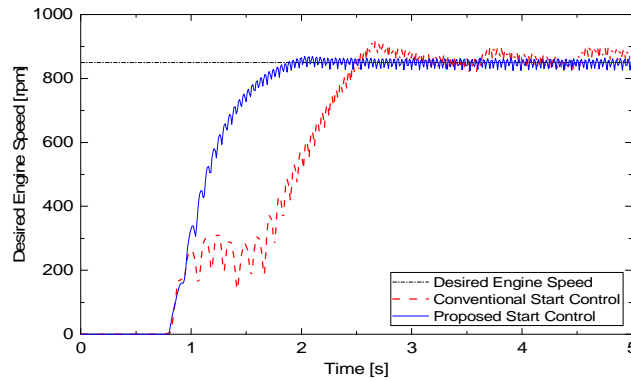


Fig. 9. Comparison of simulated engine start responses using traditional and proposed methods

7-Conclusions

In this paper, the method for starting engine without compromising the NVH performance has been introduced for micro/mild hybrid construction machines. The machine powertrain model was developed and optimized using the advanced co-simulation between AMESim and MATLAB/Simulink. This model enables users to easily explore the engine and powertrain dynamics including transient responses as well as to linearize with selected characteristics to support control design. To improve the machine efficiency, the model-based adaptive controller using PI-type neural network was built to ensure the robust engine cranking performance.

References:

1. Robinette, D. and Powell, M. Optimizing 12 Volt Start - Stop for Conventional Powertrains, SAE Int. J. Engines, December 2011, 4(1), 850-860, doi:10.4271/2011-01-0699.
2. Kum, D., Peng H. and Bucknor, N. K. Control of Engine-Starts for Optimal Drivability of Parallel Hybrid Electric Vehicles, J. Dyn. Sys., Meas., Control, March 2013, 135(2).
3. Park, K. S., Kim, S. I. and Jeong H. J. Low Idle Control System of Construction Equipment and Automatic Control Method Thereof, US patent, October 2013, US 2013/0289834 A1.
4. Frelich, T. A. Autoadaptive Engine Idle Speed Control, US patent, February 2014, US 2014/0053801 A1.
5. Truong, D. Q. and Ahn, K. K. Force control for hydraulic load simulator using self-tuning grey predictor – fuzzy PID, Journal of IFAC, Mechatronics, March 2009, 19(2), 233-246.
6. Rakopoulos, C. D. and Giakoumis, E. G. Diesel engine transient operation: Principle of operation and simulation analysis, Springer-Verlag London Limited, Springer 2009.
7. Ipci, D. and Karabulut, H. Thermodynamic and dynamic modeling of a single cylinder four stroke diesel engine, App. Math. Modelling, March 2016, 40(5-6), 3925–3937.
8. Sindhu, R., Rao G. A. P. and Murthy, K. M. Thermodynamic modelling of diesel engine processes for predicting engine performance, Int. J. of App. Eng. and Tech., April 2014, 4(2), 101-114.
9. Truong, D. Q. and Ahn, K. K. Nonlinear black-box models and force-sensorless damping control for damping systems using magneto-rheological fluid dampers, Sens. Actuators A, Phys., June 2011, 167(2), 556-573.